

# Magnetic-Sensitive Silica Nanospheres for Controlled Drug Release

Shang-Hsiu Hu, Ting-Yu Liu, Hsin-Yang Huang, Dean-Mo Liu,\* and San-Yuan Chen\*

Department of Materials Sciences and Engineering, National Chiao Tung University,  
1001 Ta Hsueh Road, Hsinchu, Taiwan, 300, Republic of China

Received May 29, 2007. In Final Form: October 1, 2007

Recently, magnetic silica-based nanospheres have received great attention and displayed magnificent potential for bioimaging and therapeutic purposes. This study provided a way to accelerate drug release from magnetic-sensitive silica nanospheres by controlled bursting to a therapeutically effective concentration by a high-frequency magnetic field (HFMF). The magnetic-sensitive silica nanospheres were synthesized by an in situ process, with particle sizes about 50 nm and able to release specific amounts of drug in a burst manner via short exposure to a HFMF. The HFMF accelerates the rotation of magnetic nanoparticles deposited in the silica matrix with generated heat energy and subsequently enlarges the nanostructure of the silica matrix to produce porous channels that cause the drug to be released easily. By taking these magnetic-responsive controllable drug release behaviors, the magnetic silica nanospheres can be designed for controlled burst release of therapeutic agents for especially urgent physiological needs.

## I. Introduction

Nanosized silica materials with multifunctions have received great attention for drug delivery systems and biomedical applications, as they provide numerous advantages such as a biocompatible, stable, and “stealthy” alternative.<sup>1</sup> Bioactive and therapeutic molecules can be easily encapsulated and display a homogeneous distribution in the silica nanoparticles by sol–gel polymerization in ambient temperature processing, necessary for handling biologicals.<sup>2</sup> The intrinsic hydrophilicity and excellent protection of silica makes them outstanding candidates for pharmaceuticals controlling drug release, which can improve the efficiency and reduce the toxicity.

Recently, functional nanomaterials like magnetic nanoparticles or quantum dots were embedded into silica nanospheres to enhance the biomedical applications.<sup>2–6</sup> Lai et al. reported that a mesoporous silica nanosphere based controlled drug delivery system was synthesized and characterized by cadmium sulfide (CdSe) as the chemically removable caps to encapsulate drug molecules in the silica matrix, and the stimuli-release can be achieved by using the chemical release trigger to remove the caps.<sup>3</sup> Functional quantum dots not only blocked the drug release but also exhibited strong excitonic photoluminescence, so the water-based luminescent magnetic colloidal silica particles can serve as luminescent markers while attached to bioligands.<sup>5</sup> On the other hand, magnetic nanoparticles have been suggested for many biomedical applications, such as bioseparation<sup>7,8</sup> and

magnetic resonance imaging (MRI).<sup>4,9</sup> Coating the silica on those functional nanoparticles forming stable and biocompatible shell avoids the potential toxicity effect on cells,<sup>10,11</sup> and incorporation of drug molecules or dye into the silica shell can reach the aims of drug delivery or labeling cells. Such core–shell nanoparticles, reported by Yoon et al., were successfully incorporated into the cells and even move the cells by an external magnetic force.<sup>2</sup> The release studies of silica materials were extended to investigate the ordered nanostructure silica.<sup>12–15</sup> With different pore size distributions, mesoporous silica can adsorb different amounts of drug molecules and control drug release for a time period varying from hours to weeks.<sup>15</sup>

It seems a good choice to use magnetic silica nanoparticles as drug delivery materials. The magnetic nanocarriers can be driven to target a specific site by a magnetic field. While the nanocarriers arrive at the therapeutic sites, triggering the drug release becomes another important subject of practical interest. Mal et al. reported that the uptake and release of organic molecules in the mesoporous silica can be regulated via photocontrolled and reversible intermolecular dimerization of coumarin derivatives onto the pore outlets.<sup>14</sup> The pH stimuli-response controlled drug release from the hollow silica spheres was studied by coating multilayer polyelectrolyte possessed pH-sensitive properties.<sup>16</sup> Additionally, there are several methods to control the drug release in recent studies, such as ultrasound and organic modification of silica.<sup>17–19</sup> Such a transfer from sensing actuation behavior is novel, but it may be hard to reach high accuracy and sensitivity

\* Corresponding author. Telephone: 8863-5712121, ext. 31818. Fax: 8863-5725490. E-mail: sanyuanchen@mail.nctu.edu.tw (S.-Y.C.) and deanmo\_liu@yahoo.ca (D.-M.L.).

(1) Barbé, C.; Bartlett, J.; Kong, L.; Finnie, K.; Lin, H. Q.; Larkin, M.; Calleja, S.; Bush, A.; Calleja, G. *Adv. Mater.* **2004**, *16*, 1959–1966.

(2) Yoon, T. J.; Kim, J. S.; Kim, B. G.; Yu, K. N.; Cho, M. H.; Lee, J. K. *Angew. Chem., Int. Ed.* **2005**, *44*, 1068–1071.

(3) Lai, C. Y.; Trewyn, B. G.; Jeftinija, D. M.; Jeftinija, K.; Xu, S.; Jeftinija, S.; Lin, V. S. Y. *J. Am. Chem. Soc.* **2003**, *125*, 4451–4459.

(4) Lu, C. W.; Hung, Y.; Hsiao, J. K.; Yao, M.; Chung, T. H.; Lin, Y. S.; Wu, S. H.; Hsu, S. C.; Liu, H. M.; Mou, C. Y.; Yang, C. S.; Huang, D. M.; Chen, Y. C. *Nano Lett.* **2007**, *7*, 149–154.

(5) Maceira, V. S.; Correa-Duarte, M. A.; Spasova, M.; Liz-Marzán, L. M.; Farle, M. *Adv. Funct. Mater.* **2006**, *16*, 509–514.

(6) Yi, D. K.; Selvan, S. T.; Lee, S. S.; Papaefthymiou, G. C.; Kundaliya, D.; Ying, J. Y. *J. Am. Chem. Soc.* **2005**, *127*, 4990–4991.

(7) Doyle, P. S.; Bibette, J.; Bancaud, A.; Viovy, J. L. *Science* **2002**, *295*, 2237.

(8) Wang, D.; He, J.; Rosenzweig, N.; Rosenzweig, Z. *Nano Lett.* **2004**, *3*, 409–413.

(9) Seo, W. S.; Lee, J. H.; Sun, X. M.; Suzuki, Y.; Mann, D.; Liu, Z.; Terashima, M.; Yang, P. C.; McConnell, M. V.; Nishimura, D. G.; Dai, H. *Nat. Mater.* **2006**, *5*, 971–976.

(10) Shchipunov, Y. A. *J. Colloid Interface Sci.* **2003**, *268*, 68–76.

(11) Lu, Y.; Yin, Y.; Mayers, B. T.; Xia, Y. *Nano Lett.* **2002**, *2*, 183–186.

(12) Lai, C. Y.; Trewyn, B. G.; Jeftinija, D. M.; Jeftinija, K.; Xu, S.; Jeftinija, S.; Lin, V. S. Y. *J. Am. Chem. Soc.* **2003**, *125*, 4451–4459.

(13) Vallet-Regí, M.; Rámila, A.; del Real, R. P.; Pérez-Pariente, J. *Chem. Mater.* **2001**, *13*, 308–311.

(14) Mal, N. K.; Fujiwara, M.; Tanaka, Y. *Nature* **2003**, *421*, 350–353.

(15) Andersson, J.; Rosenholm, J.; Areva, S.; Lindén, M. *Chem. Mater.* **2004**, *16*, 4160–4167.

(16) Zhu, Y.; Shi, J.; Shen, W.; Dong, X.; Feng, J.; Ruan, M.; Li, Y. *Angew. Chem., Int. Ed.* **2005**, *44*, 5083–5087.

(17) Giri, S.; Trewyn, B. G.; Stellmaker, M. P.; Lin, V. S. Y. *Angew. Chem., Int. Ed.* **2005**, *44*, 5038–5044.

(18) Kim, H. J.; Matsuda, H.; Zhou, H.; Honma, I. *Adv. Mater.* **2006**, *18*, 3083–3088.

(19) Muñoz, B.; Rámila, A.; Pérez-Pariente, J.; Díaz, I.; Vallet-Regí, M. *Chem. Mater.* **2003**, *15*, 500–503.

in therapeutic dosing as a burst-controlled drug delivery system, since the actuating-to-mechanical action is a function of kinetic and dynamic mechanism. A real-time burst control of drug release needs a quickly responsive drug release system to “inject” a precise amount of drug when the body needs it. In order to promote the application of stimuli-response, development of stimuli-response nanocarriers to achieve immediate, convenient response and the accurate release is essential, and this is the major objective of this investigation.

The use of a magnetic field to control drug release from a polymeric matrix was previously developed.<sup>20–23</sup> Through applying an oscillating magnetic field, the magnetic-alginate microspheres were able to release insulin in a pulsatile manner.<sup>23</sup> On the other hand, the heat energy produced by different levels of frequency was used in several applications, such as shape-memory polymer, hyperthermia in gene transfer, and cancer therapy.<sup>24–26</sup> Recently, a polyelectrolyte microcapsule embedded with Co/Au used external magnetic fields of 100–300 Hz to modulate its permeability.<sup>27</sup> However, little investigation has addressed the controlled drug release via magnetic nanocarriers under a high-frequency magnetic field (HFMF). High-frequency magnetic field is believed to accelerate the rotation or oscillation of magnetic particles more intensively and effectively than low-frequency magnetic field,<sup>27</sup> which, according to our understanding, is able to control drug release in terms of dosing characteristics and precision and can compatibly meet immediate physiological needs. Here, we reported the synthesis of a controlled drug release system that is based on the magnetic-sensitive silica nanospheres and is stimuli-responsive through a HFMF to burst release the guest molecules from the matrix.

## II. Experimental Section

**II.1. Synthesis of the Magnetic Silica Nanospheres.** The synthesis of magnetic silica nanospheres has been reported previously.<sup>28</sup> In this study, a sol–gel process was used to encapsulate the drug molecules within the silica matrix, resulting in a composite gel with therapeutic agents being homogeneously distributed in the gel.<sup>1</sup> In brief, a silica sol was prepared by mixing silicon tetraethoxide (TEOS), 2 N HCl, and ethanol in the ratio of 41.6 g/10 mL/12 mL at room temperature. After aging for 2 h, the solution was mixed with Fe(NO<sub>3</sub>)<sub>3</sub>·9H<sub>2</sub>O with different molar ratios of Si/Fe = 10/1, 5/1, 2/1, and 1/1. When Fe(NO<sub>3</sub>)<sub>3</sub>·9H<sub>2</sub>O was completely dissolved in the solution, the solution exhibited a clear, brown color, followed by adding the ibuprofen (as a model drug) into the solution. Diluted NaOH solution was added dropwise to keep the pH of the mixed solution at ~2.7. During the dropwise addition, the iron ions were partially hydrolyzed and deposited with the silica. After the silica nanospheres were formed, the solution was washed by the deionized water three times to remove residues from the surface of the nanospheres. The loading efficiency (LE) of ibuprofen is about 23% as quantitatively determined by UV, the loading capacity is 6.42 × 10<sup>-4</sup> mmol/g in the silica matrix.

**II.2. Characterizations.** The backscattering geometry of Raman spectra using 632 nm of a He–Ne laser was focused through an Olympus microscope with a 100× lens to give a spot size of 1 μm. The spectrum was obtained over a 40-s acquisition time and averaged over three accumulations. X-ray diffractometry (XRD, M18XHF, Mac Science) was used to identify the crystallographic phase of iron oxide nanoparticles, at a scanning rate of 6° 2θ per min over a range of 2θ from 15° to 70°. The magnetization of the magnetic silica nanospheres was measured by a superconducting quantum interference device (SQUID, MPMS-XL7) at 298 K and ±6000 G applied magnetic field. The morphologies of silica nanospheres were examined using field emission scanning electron microscopy (FE-SEM, JEOL-6500, Japan) and transmission electron microscopy (TEM, JEM-2010). BET analysis was measured using N<sub>2</sub> gas absorption isotherms at 77 K, and the pore size were calculated following the approach by Barrett, Joyner, and Halenda (BJH). The nanospheres were dried at 80 °C under vacuum for 1 day before BET analysis, and then the sample was degassed for 150 °C and 2 h following BET analysis.

**II.3. Drug Release Characterization.** A high-frequency magnetic field (HFMF) with 50–100 kHz was applied to the magnetic silica nanospheres to investigate the drug release behavior. The temperature of HFMF generator was controlled by cycling cooling water at 25 °C. The coil of the HFMF has eight loops, and the strength of the magnetic field (*H*) is 2.5 kA/m. The drug release behavior from the magnetic silica nanospheres was measured in 20 mL of phosphate-buffered saline per sponge cube (pH 7.4). To measure the concentration of drug release, 1.5 mL of PBS medium with the dispersed nanospheres was taken out and separated by centrifuge at 6000 rpm. The clear solution without nanospheres was used to estimate the concentration of drug release. UV–visible spectroscopy (Agilent, 8453 UV-visible spectrophotometer) was used for characterization of the absorption peak at 264 nm to determine ibuprofen concentration. The nanospheres were absent and did not affect the measurements.

## III. Results and Discussion

**III.1. Preparation of Nanospheres.** In the synthesis of sol–gel silica nanoparticles, particle formation with a controllable size is technically important while the resulting controlled release property is preserved. The size of nanoparticles is controlled by the viscosity and surface tension of sol–gel solution, as well as reaction kinetics. To prepare nanoparticles and accurately control the release, we developed a simple method that is able to produce the Si/Fe nanoparticles via the sol–gel process. Water-soluble iron salts and silica precursors were dissolved and mixed together to form a homogeneous and clear solution. With control over the solution pH, the hydrolysis of tetraethoxyorthosilicate (TEOS) was carried out in the solution, and then uniform particles were formed. The resulting nanoparticles shown the Figure 1, ranging from 40 to 60 nm in diameter, can be produced by varying the molar ratio of the Si/Fe, and it was found that the particle size increased with increasing Si/Fe ratio. In the process of the formation of nanoparticles, the solution became black in the beginning, which means that iron salts transformed into iron oxide first, and later, the solution gradually changed from black to gray, implying that silica precursors subsequently attach on the surface. As a result, the iron oxide nanoparticles were easily coated with the silica, suggesting that the hydrolysis and deposition of TEOS hindered the growth of the iron oxide nanoparticles. The TEM photo in Figure 1c shows that there were several darker dots in the nanospheres, suggesting the iron oxide embedding in the nanospheres, as confirmed later by the Raman analysis. On the other hand, the resulting samples can dispersed well in the PBS solution (pH 7.4) for 24 h, suggesting that the nanospheres were stable under high salt concentration (physiological conditions). So there was no stabilizer in this system.

(20) Kost, J.; Wolfrum, J.; Langer, R. *J. Biomed. Mater. Res.* **1987**, *21*, 1367–1373.

(21) Edelman, E. R.; Kost, J.; Bobeck, H.; Langer, R. *J. Biomed. Mater. Res.* **1985**, *19*, 67–83.

(22) Kost, J.; Noecker, R.; Kunica, E.; Langer, R. *J. Biomed. Mater. Res.* **1985**, *19*, 935–940.

(23) Saslawski, O.; Weingarten, C.; Benoit, J. P.; Couvreur, P. *Life Sci.* **1988**, *42*, 1521–1528.

(24) Mohr, R.; Kratz, K.; Weigel, T.; Lucka-Gabor, M.; Moneke, M.; Lendlein, A. *Proc. Natl. Acad. Sci. U.S.A.* **2006**, *103*, 3540–3545.

(25) Zintchenko, A.; Ogris, M.; Wagner, E. *Bioconjugate Chem.* **2006**, *17*, 766–772.

(26) Jordan, A.; Scholz, R.; Wust, P.; Föhling, H.; Felix, R. *J. Magn. Magn. Mater.* **1999**, *201*, 413–419.

(27) Lu, Z.; Prouty, M. D.; Guo, Z.; Golub, V. O.; Kumar, C. S. S. R.; Lvov, Y. M. *Langmuir* **2005**, *21*, 2042–2050.

(28) Han, Y. S.; Matsumoto, H.; Yamanaka, S. *Chem. Mater.* **1997**, *9*, 2013–2018.



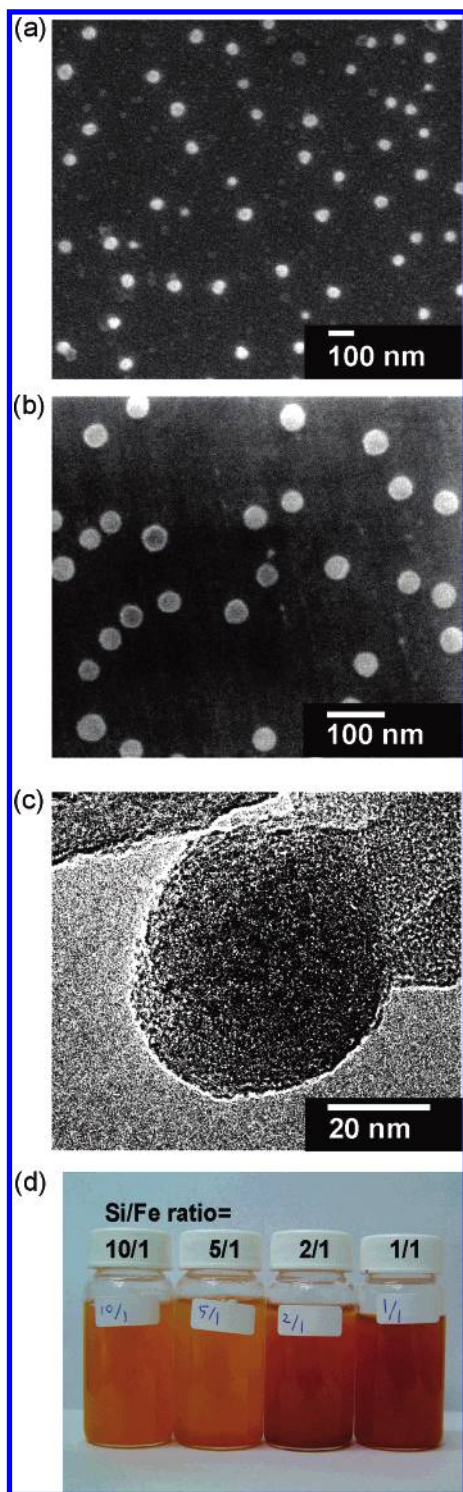


**Figure 1.** Scanning electron microscopy images of silica-based nanospheres: (a) Si/Fe = 1/1 and (b) Si/Fe = 10/1. The diameters of nanospheres ( $\text{Fe}_3\text{O}_4$ @silica) were distributed in the range of 40–60 nm. (c) Transmission electron microscope images of Si/Fe = 1/1 nanospheres. (d) The photograph shows nanospheres that were dispersed in the PBS solution for 1 day, after a pretreatment of ultrasonication.

**III.2. Characterization of Nanospheres.** The Raman spectra of the nanospheres with different Si/Fe molar ratios were measured at ambient conditions, as shown in Figure 2a. The silica possesses Raman bands at 488, 600, and 819  $\text{cm}^{-1}$ . The broad bands at 600 and 488  $\text{cm}^{-1}$  were attributed by the D2 and D1 defect modes, which were ascribed to tri- and tetracyclosoloxane rings from

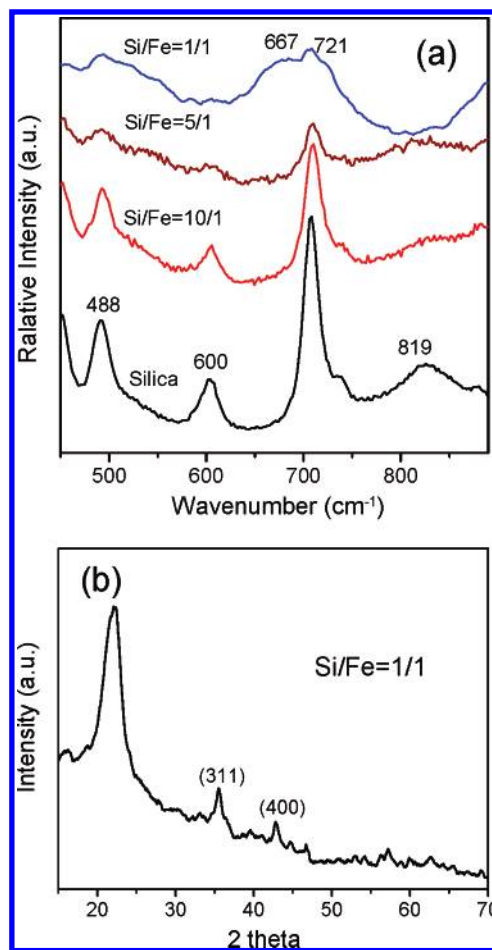


**Figure 2.** (a) The Raman spectra of the nanospheres with different Si/Fe molar ratios. (b) XRD pattern of Si/Fe = 1/1 nanospheres.

condensation of surface hydroxyls.<sup>29</sup> The symmetrical Si–O–Si stretching mode has assigned the band at 819  $\text{cm}^{-1}$ . The changes in the silica Raman bands at 600 and 488  $\text{cm}^{-1}$  are not very obvious for nanospheres with different Si/Fe ratios. However, with increasing concentration of the iron salts, the Raman spectra showed the presence of the iron oxide, i.e., 667  $\text{cm}^{-1}$ , which is assigned to the characteristic band of  $\text{Fe}_3\text{O}_4$ , a symmetrical peak attributed to the vibration modes consisting of stretching of oxygen atoms along Fe–O bonds. In addition, the characteristic peaks for  $\gamma$ - $\text{Fe}_2\text{O}_3$  are also present at 721  $\text{cm}^{-1}$  and a weaker band at 667  $\text{cm}^{-1}$ .<sup>30</sup> The results indicated that the iron oxide was also developed as a phase-pure entity in the nanospheres, while the Si/Fe ratio is increased to 1/1.

As shown in Figure 1c, the iron oxides present in the TEM photo show an agglomeration size of about 2–4 nm, indicating that the primary size of the resulting iron oxide can be in the range of a fraction of 1 nm, which is much smaller than those reported in literature, typically ranging from 5 to 10 nm in dimension. This suggests the highly amorphous nature of the iron oxide nanoparticles being synthesized in this study. We do not clearly understand why the iron oxide particles developed in such small dimensions, but the presence of the silica matrix may have a profound effect, since it is possibly developing Si–O–Fe bonds in either chemical or physical nature during the synthesis, which inhibits the growth of the iron oxide crystals

(29) Maxim, N.; Overweg, A.; Kooyman, P. J.; van Wolput, J. H. M. C.; Hanssen, R. W. J. M.; van Santen, R. A.; Abbenhuis, H. C. L. *J. Phys. Chem. B* **2002**, *106*, 2203–2209.

(30) Long, J. W.; Logan, M. S.; Rhodes, C. P.; Carpenter, E. E.; Stroud, R. M.; Rolison, D. R. *J. Am. Chem. Soc.* **2004**, *126*, 16879–16889.

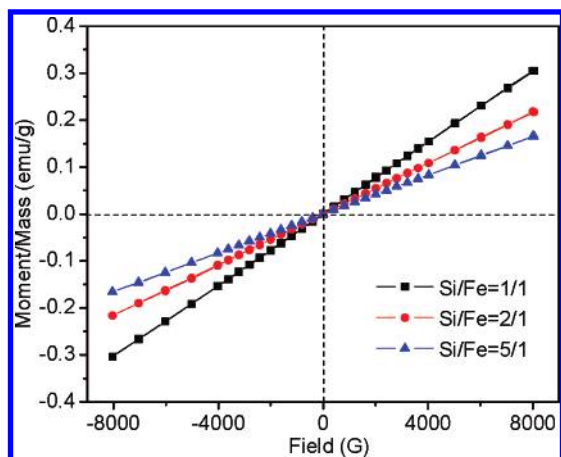


**Figure 3.** Field-dependent magnetization curve of silica-based nanospheres.

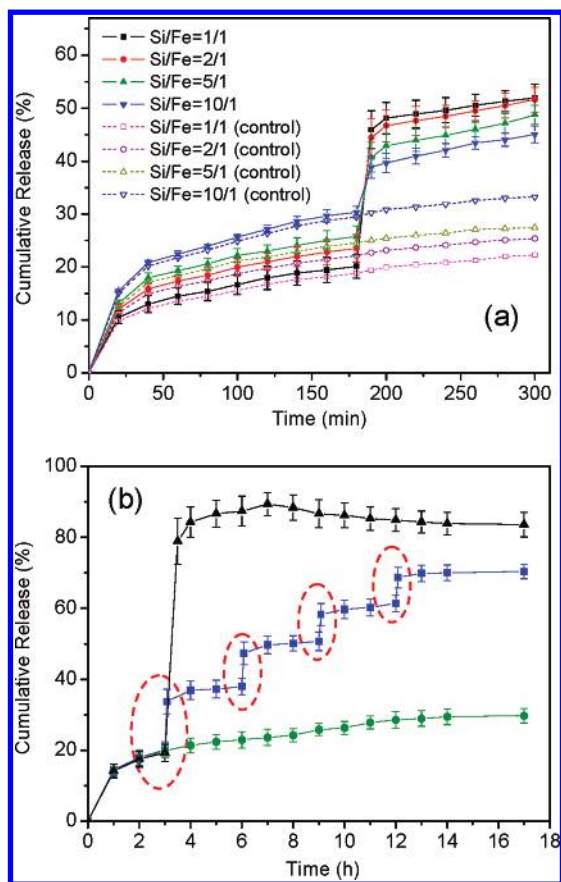


**Figure 4.** (a) Drug-release profiles of silica nanospheres were triggered by a 10-min high-frequency magnetic field (HFMF), from minute 180 to 190 (solid line). The control group of silica nanospheres without magnetic iron incorporation is also shown (dash line). (b) Cumulative release of drug (ibuprofen) from silica nanospheres (Si/Fe = 1/1) without magnetic stimulation (green circles), silica nanospheres after a 30-min exposure to magnetic stimulation (black triangles), and silica nanospheres with magnetic stimulation of 50 kHz applied at the four specific times indicated by the circled data points (blue squares).

once being nucleated in the silica matrix. On this basis, the resulting iron oxide nanoparticles are amorphous and hard to identify by XRD analysis, but in contrast, Raman analysis seems to provide a powerful tool in structural identification, and we have confirmed this experimentally. Upon increasing the content of iron precursor, i.e., in the case of Si/Fe = 1/1 only, the inhibition of crystal growth can be reduced considerably, making the iron

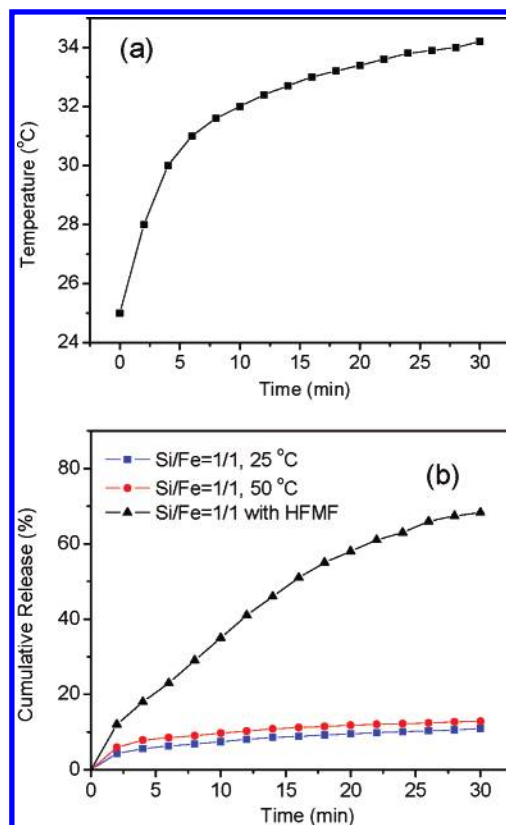


**Figure 5.** (a) Temperature increase curve of Si/Fe = 1/1 nanospheres when applying the HFMF. (b) The drug release behaviors of Si/Fe = 1/1 nanospheres under HFMF, heating to 50 °C and room temperature for 30 min.

oxide nuclei grow into larger particles, rendering the resulting crystalline structure XRD detectable (Figure 2b). The XRD pattern of Si/Fe = 1/1 nanosphere exhibited the crystalline phases of iron oxide nanoparticles according to JCPDS [85-1436], and one more peak at  $2\theta \sim 23^\circ$  was observed and can be identified as the semicrystalline silica. In Figure 3, the magnetization–magnetic field curves for all the Si/Fe nanospheres display similar shape with paramagnetic properties. The nanospheres exhibit higher magnetic strength with lower Si/Fe molar ratio, and thus, Si/Fe = 1/1 possesses the strongest magnetic strength among all compositions, which is clearly a Fe-concentration dependent behavior; i.e., the higher the Fe concentration in the nanospheres, the higher the magnetic strength results.

**III.3. Magnetic-Field-Controlled Drug Release.** The drug (ibuprofen) release profile from the nanospheres without and with the use of the magnetic stimulation is demonstrated in Figure 4a. Ibuprofen-containing (1 wt %) nanospheres were used in PBS buffer solution for all the drug-release experiments. Under the condition of no magnetic field, the nanospheres with different Si/Fe ratios showed almost identical release profiles but different amounts of drug in the first 3 h of release, even though they have similar particle sizes. The nanospheres of higher Si/Fe ratio (Si/Fe = 10/1) generally showed faster drug release than those of lower ratio (Si/Fe = 1/1). To investigate the diffusion mechanism of the drug from the nanoparticles, the drug release profile can be characterized using the equation:

$$M_t/M = kt^n$$

where  $M_t$  is the mass of drug released at time  $t$ ,  $M$  is the mass released at infinite time,  $k$  is a rate constant, and  $n$  is a characteristic

**Table 1. Physical Properties of Magnetic-Sensitive Silica Nanospheres for Different Times of HFMF Treatment**

Si/Fe	surface area <sup>a</sup> (m <sup>2</sup> /g)			pore volume <sup>b</sup> (cm <sup>3</sup> /g)			average pore diameters (nm)		
	0 min	5 min	30 min	0 min	5 min	30 min	0 min	5 min	30 min
1/1	41	42	69	0.067	0.067	0.127	6.5	6.5	7.4
5/1	45	45	47	0.079	0.079	0.088	6.7	6.7	6.8
10/1	48	48	48	0.083	0.083	0.084	6.8	6.8	6.8

<sup>a</sup> Multipoint BET method; replicate analyses are 5%. <sup>b</sup> BJH method, adsorption isotherm.

exponent related to the mode of transport of the drug molecules.<sup>31</sup> The diffusion parameters (i.e.,  $n$  and  $k$ ) can be obtained through a log-log analysis of the above equation under the condition of  $M_t/M < 0.6$ . The values of rate constant  $k$  for the nanoparticles with different Si/Fe ratios were then determined and the  $k$  values were found to decrease in the order of 10/1 ( $k = 4.3$ ) > 5/1 ( $k = 3.7$ ) > 1/1 ( $k = 2.6$ ), indicating a lower diffusion kinetic for lower Si/Fe ratio. The results indicated that the nanospheres of lower Si/Fe ratio, e.g., Si/Fe = 1/1, should more effectively inhibit drug diffusion than that of higher Si/Fe ratio. This finding suggests that the low-Si/Fe nanospheres may be characterized to (1) possess more barriers for drug diffusion, (2) have a denser structure, and/or (3) provide more affinity to the drug molecules than the high-Si/Fe nanospheres.

A burst release was detected right after the high-frequency magnetic field (HFMF) was applied to the nanospheres after the first 3 h of slow release, for a duration of 10 min. After then, the release profile restores to a slow profile, as the profile disclosed in the first 3 h, once the field was removed. It is interesting to realize that the low-Si/Fe (1/1) nanospheres exhibit the strongest burst, as high as 46%, among all compositions, and the burst amount decreased with increasing Si/Fe ratio. The results suggest that the amount of burst release under HFMF may be related with the nanospheres' magnetic properties. For example, Si/Fe = 1/1 nanospheres possessed the higher magnetic strength in the same magnetic field (from SQUID analysis, Figure 3), and they displayed a stronger burst than the other compositions. On the other hand, the release profiles were restored immediately and completely after removal of the HFMF stimuli. In other words, the drug release behaviors of nanospheres can be changed from a steady-state, slow profile to a burst profile immediately after a short time exposure to the HFMF stimuli, and those profiles can recover rapidly to their original state upon removing the magnetic field. This observation suggests that the variation in the nanostructure of the Si/Fe nanospheres is physically reversible, and it is believed that the magnetically induced deformation of the nanosphere as a result of the oscillation or vibration of the embedded magnetic nanoparticles can be elastic. This elastic deformation ensures a long-term, reliable controlled release of the drug. In addition, the fast response of the nanospheres with respect to burst release of drug right after subjecting to the HFMF stimulus provides greater potential for an in-time drug release for medical applications.

Figure 4b shows that the drug-loaded nanospheres were actuated by applying an external high-frequency magnetic field (HFMF) of 50 kHz for 5 min at four specific times (blue squares). After magnetic excitation, a significant increase in the amount of drug released was observed. The result implied that the drug molecules in the nanospheres exactly followed the signals switching from burst to slow release for each operation. While applying a HFMF, the amounts of drug released can increase instantly, and under suitable control, the drug concentration can reach the therapeutic window within a short time period. A control

experiment (green circles) was also carried out to display that the model drug did not exhibit a significant release; however, after a 30-min exposure to the HFMF, as shown in Figure 4b (black triangle), considerable drug was released from the nanospheres. After removing HFMF, the drug still released faster compared with the normal release rate; in contrast, a short exposure time of 5 min of HFMF (blue square) allowed the nanostructure or nanopores to be recoverable. In order to directly compare the porosity of the nanospheres without HFMF and for those under short time exposure to HFMF, the nanospheres were immersed in the buffer solution, which was subjecting to the same conditions as those nanospheres treated under HFMF. As shown in Table 1, after applying 0 and 5 min of HFMF to the silica nanospheres, there is nearly no difference in the surface areas, pore volumes, or peak pore diameters, but drug release rates can obviously increase, implying that the structures are not severely changed with short time exposure to HFMF. A long-time HFMF (30 min) exposure caused unrecoverable pore enlargement, as further confirmed with increased porosity. This suggests that a long exposure to the HFMF may cause either a large or plastic deformation or fatigue of the nanostructure from the original state. However, either short-term or long-term exposure may be used on the basis of the clinical needs for the best therapeutic strategy.

The influence of temperature rise due to field stimulus on the nanospheres was also considered. During the application of HFMF for 30 min, a 9–10 °C increment in temperature for Si/Fe = 1/1 was observed, as shown in the Figure 5a. The sample with identical composition of Si/Fe = 1/1 was heated to 50 °C for 30 min and the drug release behavior was monitored and compared with the behavior in the presence of HFMF (Figure 5b). It is clear that the influence of temperature (even through it is raised due to magnetically induced operation) on the release behavior from the nanospheres is negligibly small. The silica is not a thermosensitive material, and it is believed that the nanostructure is not changed as a result of a small temperature rise. Thus, one can conclude that the temperature effect on the release behaviors of the nanospheres is negligible; in contrast, the influence of the HFMF is the major factor resulting in burst release.

In order to investigate the change in the pore structure of the nanospheres, the HFMF was applied for a long time period to produce unrecoverable pores. Nitrogen-adsorption measurements were conducted to measure the change in porosity (or pore size evolution) of the nanospheres, as illustrated in Figure 6a, which shows the nitrogen-adsorption isotherm for the nanospheres before and after applying the HFMF for a time period of 30 min. As-synthesized nanospheres showed a specific surface area of 41 m<sup>2</sup> g<sup>-1</sup> and a total pore volume of 0.067 cm<sup>3</sup> g<sup>-1</sup>. After being subjected to the HFMF, the surface area and total pore volume of the nanospheres significantly increased to 69 m<sup>2</sup> g<sup>-1</sup> and 0.127 cm<sup>3</sup> g<sup>-1</sup>, respectively, indicating that the nanostructure of the nanospheres can be manipulated with a noncontact high-frequency magnetic field. The average pore diameter of the nanospheres is determined to be 6.5 and 7.4 nm without and with HFMF, respectively. The average pore size only slightly changed.

(31) Ritger, P. L.; Peppas, N. A. *J. Controlled Release* **1987**, *5*, 37–42.



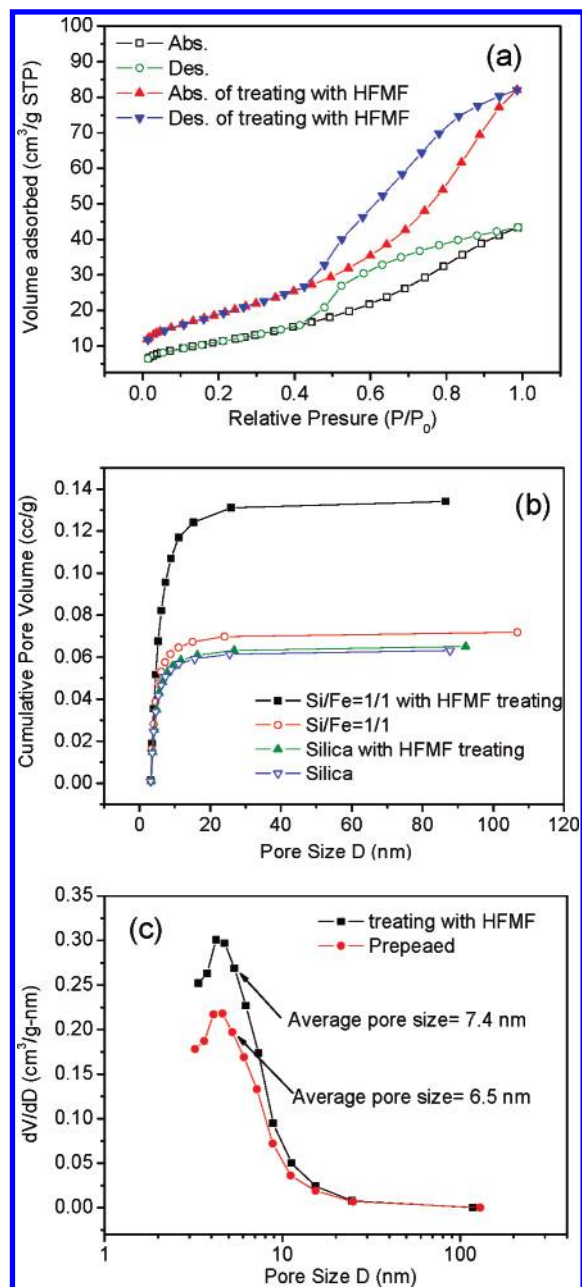


**Figure 6.** (a) BET measurements of silica nanospheres treated with HFMF for 30 min and without HFMF treatment. (b) Cumulative pore volumes and (c) pore size distribution of silica nanospheres with and without HFMF treatments.

However, Figure 6b shows that the amount of cumulative pores increased considerably from 5 to 11 nm after long-term exposure

to the HFMF, and the pore size distribution is also shown in Figure 6c. The changes in the porosities evidenced that a noncontact HFMF can transfer kinetic energy into the nanospheres, and while the magnetic nanoparticles received the energy, the nanospheres deformed their inner structures and subsequently produced or enlarged those pores in the nanospheres. Moreover, the HFMF-induced energy can cause the vibration to pump the drug out and even change the nanostructures of these nanospheres. Although the amount of pores increased after the long time exposure of HFMF, the porosity of the nanospheres for short time (10 min) exposure increased less significantly, implying that those pores showed recoverable behaviors. Accordingly, the result of the drug release behaviors for 5 min exposure of HFMF in Figure 4b (blue squares) also exhibited recoverable behaviors, so the nanospheres could block the continued release of drug molecules after removing the HFMF stimulus.

The exact mechanism of burst release is still not clear. However, from the variation of pore size distribution in the nanoparticles before and after magnetic field stimulus over different time periods, we believe that the silica matrix may keep the same structure during the field stimulus but that the primary particles of iron oxide may be subjected to rearrangement in a confined space similar to the size of the agglomerated particles shown in Figure 1c. Therefore, variation in the microporous region (becoming bigger after long-term field stimulus) due to rearrangement of the primary particles may provide more plausible explanation, as has been confirmed from the BET analysis. From the cumulative pore volumes and pore distributions in Figure 6b,c, the regions with largest change in the pore volume-pore size profile is from 2 to 5 nm, which exactly correlated with the size of the agglomerates in the nanospheres.

#### IV. Conclusions

The magnetic-sensitive nanospheres were prepared through an in situ process using iron salts and silica precursors, with particles size about 50 nm in diameter. The production of pores in the nanospheres can be significantly increased in a short time by a noncontact high-frequency magnetic field (HFMF). With this behavior, these magnetic-sensitive silica nanospheres can precisely release drugs and bioactive molecules in desired amounts by using magnetic simulation of the drug-loaded nanospheres. In addition, silica nanospheres are versatile for many further applications because they can be easily derivatized to bind to targeted agents such as proteins or antibodies, which we are actively pursuing in this lab. It is suggested that these nanospheres with precise magnetic sensitivity are promising to serve as a carrier for other drug delivery applications.

LA701570Z